ORIGINAL ARTICLE

Morphometric analysis program and quantitative positron emission tomography in presurgical localization in MRI-negative epilepsies: a simultaneous PET/MRI study

Kun Guo[1] · Jingjuan Wang[1] · Zhenming Wang[1] · Yihe Wang[2] · Bixiao Cui[1] · Guoguang Zhao[2] · Jie Lu[1,3]

Abstract

Purpose To evaluate morphometric analysis program (MAP) and quantitative positron emission tomography (QPET) in epileptogenic zone (EZ) identification using a simultaneous positron emission tomography/magnetic resonance imaging (PET/MRI) system in MRI-negative epilepsies.

Methods Seventy-one localization-related MRI-negative epilepsies who underwent preoperative simultaneous PET/MRI examination and surgical resection were enrolled retrospectively. MAP was performed on a T1-weighted volumetric sequence, and QPET was analyzed using statistical parametric mapping (SPM) with comparison to age- and gender-matched normal controls. The sensitivity, specificity, positive predictive value (PPV), and negative predictive value (NPV) of MAP, QPET, MAP+QPET, and MAP/QPET in EZ localization were assessed. The correlations between surgical outcome and modalities concordant with cortical resection were analyzed.

Results Forty-five (63.4%) patients had Engel I seizure outcomes. The sensitivity, specificity, PPV, and NPV of MAP were 64.4%, 69.2%, 78.3%, and 52.9%, respectively. The sensitivity, specificity, PPV, NPV of QPET were 73.3%, 65.4%, 78.6%, and 58.6%, respectively. MAP+QPET, defined as two tests concordant with cortical resection, had reduced sensitivity (53.3%) but increased specificity (88.5%) relative to individual tests. MAP/QPET, defined as one or both tests concordant with cortical resection, had increased sensitivity (86.7%) but reduced specificity (46.2%) relative to individual tests. The regions determined by MAP, QPET, MAP+QPET, or MAP/QPET concordant with cortical resection were significantly associated with the seizure-free outcome.

Conclusion QPET has a superior sensitivity than MAP, while the combined MAP+QPET obtained from a simultaneous PET/MRI scanner may improve the specificity of the diagnostic tests in EZ localization coupled with the preferable surgical outcome in MRI-negative epilepsies.

Keywords Epilepsy · PET/MRI · MAP · Quantitative PET · Localization

---

Kun Guo and Jingjuan Wang contributed equally to this article

---

This article is part of the Topical Collection on Neurology

✉ Jie Lu
imaginglu@hotmail.com

1 Department of Radiology and Nuclear Medicine, Xuanwu Hospital Capital Medical University, Beijing 100053, China

2 Department of Neurosurgery, Xuanwu Hospital, Capital Medical University, Beijing, China

3 Key Laboratory of Magnetic Resonance Imaging and Brain Informatics, Beijing, China

Introduction

For magnetic resonance imaging (MRI)-negative intractable focal epilepsy patients, identifying a subtle abnormality that was previously undetected helps to provide an opportunity for surgical treatment. Longitudinal studies in MRI-negative focal epilepsy patients showed that resected surgery offers the potential for long-term seizure control [1, 2], which encouraged researchers to use postprocessing imaging analysis to identify more potential epileptogenic zone (EZ).

In morphometric analysis program (MAP), one of many MRI postprocessing imaging analyses, several researchers have demonstrated that MAP could be helped detect subtle abnormalities of focal cortical dysplasia (FCD) in

MRI-negative surgical candidates [3–5]. However, the false positive of MAP methodology caused by imaging artifacts, registration errors, and nonepileptic variants may lead to multiple regions on the output maps, which may resemble epileptogenic lesions. The focal hypometabolism foci shown on interictal ^{18}F-fluorodeoxyglucose (^{18}F-FDG) positron emission tomography (PET) was associated with EZ [6, 7]. ^{18}F-FDG PET has been widely used in preoperative localization of drug-resistant epilepsy with a negative MRI [8, 9]. Quantitative PET (QPET) analysis using statistical parametric mapping (SPM) can help to provide objective data, and improve the diagnostic of PET, especially in the patients with normal vision on PET scans [10–13]. There are less data in the literature on the sensitivity and specificity of combined postprocessing imaging with localization-related MRI-negative epilepsies.

The combination of MAP and QPET imaging analysis facilitated the objective identification of epileptogenic abnormalities that have been reported by Lin. et al. [14]. However, the non-simultaneous acquisition in different machines and times and various motion artifacts may lead to potential biases in the subtle EZ localization. In the present study, ^{18}F-FDG PET and MRI images were obtained from a simultaneous PET/MRI; the sensitivity, specificity, positive predictive value (PPV), and negative predictive value (NPV) of MAP, QPET, MAP + QPET, and MAP/QPET in detection EZ were evaluated. Moreover, whether the concordance between the regions identified by MAP and QPET and the surgical resection associated with seizure outcomes was explored.

Material and methods

Patients and healthy controls

This retrospective study was permitted by the Research Ethics Committee of the Capital Medical University of Xuanwu Hospital. Written informed consent was obtained from each participant.

Patients were included if they had (1) no blurring of the gray-white matter junction, no abnormally thickened cortex, no decreased cortical T1 signal intensity, no increased cortical T2/FLAIR signal intensity, and no T2/FLAIR subcortical abnormalities on MRI; (2) a preoperative simultaneous ^{18}F-FDG PET/MRI scan; (3) received a comprehensive presurgical evaluation including seizure semiology, video-electroencephalography (V-EEG), neuroimaging, and intracranial EEG (IEEG); (4) postoperative follow-up of over 12 months; and (5) a postoperative MRI or CT scan. Patients were excluded if they had (1) poor PET/MRI quality hindering clinical read or (2) poor PET/MRI quality causing significant registration errors in the data processing

procedures and also (3) patients who diagnosed with crossed cerebellar diaschisis.

The surgical site was determined by a multidisciplinary conference including seizure semiology, neuropsychologic examination, long-term ictal and interictal scalp electroencephalography surveillance, and anatomic and functional neuroimaging studies. For the patients with negative neuroimaging results or dis-concordant neuroimaging findings, IEEG was critical for surgical sites confirmation. None of the patients had intraoperative or perioperative complications, and the preoperative antiepileptic regimen was continued for all patients in the postoperative period.

Available microscopic slides from surgical resections were reviewed by a dedicated neuropathologist. Pathology results were classified according to the International League Against Epilepsy classification [15].

Seizure outcomes were categorized 1 year after surgery by the Engel Epilepsy Surgery Outcome Scale [16]. Surgical outcome was then categorized as Engel I (seizure-free) and Engel II–IV (non-seizure-free). The demographic and clinical characteristics of all participants are presented in Table 1.

Twenty-two age- and gender-matched healthy controls (HCs) (mean age, 29.32 ± 5.65 years, range, 17–39 years; 11 males) were enrolled. All HCs were free of psychiatric or neurologic disorders on the basis of a health screening measure.

PET/MRI acquisition

Interictal ^{18}F-FDG PET and MRI data were simultaneously obtained using a simultaneous TOF-PET/MR scanner (SIGNA, GE Healthcare, WI, USA). The patients fasted at least 6 h, and the level of fasting blood glucose was lower than11.1 mmol/L. ^{18}F-FDG with radiochemical purity of > 95% was produced by the unit, and the injection dosage was calculated based on the patients' body weight (3.7 MBq/kg). All patients were at rest in a dimmed environment for 40 min. Video surveillance was used to monitor the patients to exclude an ictal or postictal FDG administration. During the scanning, the subjects were instructed to keep their eyes open, and keep their head as still as possible. Three-dimension T1 brain volume imaging (3D T1 BRAVO) (repetition time (TR) = 2300 ms, echo time (TE) = 2.98 ms, angle = 9°, slices/gap = 160/0.5 mm, FOV = 256 mm, matrix size = 256 × 256, voxel size = $1.0 \times 1.0 \times 1.0$mm^3) and other structural imaging sequences for diagnosis images were immediately obtained.

Forty minutes after tracer injections, PET images were acquired with a static 10-min period. The PET bed position included a simultaneous 18-s 2-point Dixon scan for MRI. Attenuation correction, scatter correction, random correction, and dead-time correction were

Table 1 Detailed demographics and clinical data of patients

Variable	Total ($n = 71$)	Seizure-free ($n = 45$)	Non-seizure-free ($n = 26$)	P
Gender (n, %)				0.14[b]
Male	44 (62.0)	25 (55.6)	19 (73.1)	
Female	27 (38.0)	20 (44.4)	7 (26.9)	
Age (y, mean $\pm$ SD)	25.7 $\pm$ 9.4	26.0 $\pm$ 9.3	25.3 $\pm$ 9.6	0.79[a]
Age group				0.49[b]
$\geq$ 18y	57 (80.3)	35 (77.8)	22 (84.6)	
< 18 y	14 (19.7)	10 (22.2)	4 (15.4)	
Age of onset (y, mean $\pm$ SD)	13.3 $\pm$ 8.6	13.5 $\pm$ 8.3	13.0 $\pm$ 9.2	0.83[a]
Duration (y, mean $\pm$ SD)	12.3 $\pm$ 8.4	12.4 $\pm$ 8.7	12.1 $\pm$ 8.2	0.88[a]
Febrile convulsion (n, %)	9 (12.7)	6 (13.3)	3 (11.5)	0.83[b]
Medication (n, %)				0.72[b]
$\leq$ 2	39(54.9)	24 (53.3)	15 (57.7)	
> 2	32(45.1)	21 (46.7)	11 (42.3)	
Resection area (n, %)				0.33[b]
Frontal	13 (18.3)	10 (22.2)	3 (11.5)	
Parietal	7 (9.9)	3 (6.7)	4 (15.4)	
Occipital	1 (1.4)	0 (0)	1 (3.8)	
Temporal	39 (54.9)	26 (57.8)	13 (50)	
Multi-lobar	11 (15.5)	6 (13.3)	5 (19.2)	

SD standard deviation

[a]*t* test. [b]Pearson's chi-square test

also performed. Scanning parameters for reconstructed images were as follows: matrix size $= 192 \times 192$, voxel size $= 1.82 \times 1.82 \times 2.78$ mm^3, 89 slices. Time of flight, ordered subsets expectation maximization (TOF-OSEM) algorithm was used for PET image reconstruction, the detailed parameters were the following: 3 iterations, 32 subsets, and full width at half maximum of a Gaussian filter of 3.0 mm.

MRI postprocessing

MAP was performed on 3D T1 BRAVO images using an in-house code in MATLAB. The computed output consists of 3 volumetric statistical maps, called the junction, extension, and thickness maps. A blinded reviewer used the *z* score threshold of 4 to identify candidate MAP positive regions on the junction file, an accompanying region on the extension file ($z > 6$), and the thickness file ($z > 4$). The choice of *z* score threshold was consistent with previous literature [3]. Candidate MAP positive regions were searched in the whole brain. All candidate MAP positive regions were then addressed by two experienced neuroradiologists, who conducted a corresponding focused re-review of the pre-operative clinical MRI (with 3D T1 BRAVO, T2-weighted FLAIR, and turbo spin-echo sequences). If they have any opinions, a third neuroradiologist needed to determine. The MAP result was classified as concordant with cortical resection if the abnormal area included the resection site;

otherwise, it was classified as non-concordant with cortical resection.

QPET analysis

All imaging data were preprocessed in SPM12 (http://www.fil.ion.ucl.ac.uk/spm/software/spm12) and an in-house code in MATLAB. Glucose metabolism from all HCs was served as the normal database. To assess the individual glucose metabolism changes, a two-sample *t* test was performed between individual patient data and the normal database, with age and gender regressed out as covariates to reduce the effects of these variables. Global nuisance effects were estimated by dividing the intensity in each image by the intensity of the cerebellum. Registered PET maps were spatially normalized to the Montreal Neurological Institute (MNI) space by the same transformation parameters from the segmentation procedure of the T1-weighted images. Pre-processed PET images in MNI space were converted to the standardized uptake value ratio (SUVr) relative to the cerebellum and then smoothed using a 6-mm full width at half maximum (FWHM) Gaussian kernel. The resulting SPM (*t*) maps were thresholded with a significance level of $P < 0.05$ without corrections. The SPM (*t*) maps were reviewed by a dedicated nuclear medicine physician to exclude the focal metabolism caused by a sulcus. If the physician has any questions, another physician is required to make a decision after consultation. The QPET result was interpreted as a normal or abnormal scan. If the SPM (*t*) maps were

abnormal, the anatomic location of abnormal metabolism was recorded. The QPET result was classified as concordant with cortical resection if the abnormal metabolic area included the resection area; otherwise, it was classified as non-concordant with cortical resection.

The two nuclear medicine physicians judged whether the MAP positive areas were located in the hypometabolism cluster on QPET results. For the combined MAP+QPET, if the results of both of the tests were concordant with cortical resection, the combined tests were considered concordant; conversely, if the result of one of the tests was non-concordant, the combined tests were considered non-concordant. For MAP/QPET, if the result of one of the tests was concordant, the tests were considered concordant; conversely, MAP/QPET was considered non-concordant if both tests were non-concordant.

Statistical analysis

All data analysis was performed with SPSS software (IBM SPSS Statistics, version 21.0). Group-level comparisons of demographic and clinical characteristics were carried out with independent sample Student's t tests, one-way analysis of variance, or chi-square tests. $P < 0.05$ was considered statistically significant. True positive (TP) was classified as imaging results concordant with surgical resection in seizure-freedom patients (Engel I); false positive (FP) was classified as imaging results concordant with surgical resection in patients with ongoing seizures (Engel II–IV). The imaging results non-concordant with surgical resection in patients with ongoing seizures were classified as true negative (TN). Such a case neuroimaging found no focal lesion, and surgery proceeded, but the patient did not improve. False negative (FN) was defined as imaging results non-concordant with the actual surgical resection in seizure-freedom patients. Sensitivity=TP/TP+FN, Specificity=TN/TN+FP, PPV=TP/TP+FP, NPV=TN/TN+FN was calculated. Associations between the regions identified by QPET and MAP concordant with cortical resection and seizure outcome at least 1 year were tested by chi-square tests.

Results

Subjects

Seventy-one epilepsy patients with a negative MRI were included. There was no significant difference between the epilepsy patients and healthy controls in age or gender ($P > 0.05$). Forty-five (63.4%) patients had Engel I seizure outcomes at 1-year follow-up. There was no significant difference between the seizure-free (Engel I) and non-seizure-free (Engel II–IV) groups in other clinical characteristics, including the age of onset, epilepsy duration, history of medication, and resection area ($P > 0.05$). The detailed demographics and clinical data of patients and healthy controls are listed in Table 1.

Surgical pathology included FCD in 48 (67.6%) patients (including FCD I in 36 cases, FCD II in 9 cases, and FCD III in 3 cases), hippocampal sclerosis (HS) in 5 (7.0%) patients, FCD associated with HS in 3 (4.2%) patients, and other pathology in 3 (4.2%) patients (ulegyria in 2 patients and ganglioglioma WHO I in one patient). Twelve (16.9%) patients had negative surgical histology.

MAP

Candidate MAP positive regions were found in 50 patients (70.4%), including 35 patients with single candidate MAP positive regions and 15 patients with multiple candidate MAP positive regions. Candidate MAP positive regions were concordant with cortical resection in 37 patients, of whom 29 patients achieved Engel I seizure outcome and eight patients with Engel II–IV seizure outcome. MAP was negative in 21 patients and localized but non-concordant with cortical resection in 13 patients, of whom 16 patients achieved Engel I seizure outcome and 18 patients with Engel II–IV seizure outcome. The sensitivity of MAP was 64.40%, specificity was 69.2%, PPV was 78.3%, and NPV was 52.9% (Table 2). Candidate MAP positive regions concordant with cortical resection were associated with favorable seizure outcomes ($P = 0.006$) (Table 3).

QPET

QPET positive regions were found in 66 patients (93.0%), including 56 patients with single sit hypometabolism and 10 patients with multiple site hypometabolism. QPET positive regions were concordant with surgical resection in 42

Table 2 Sensitivity, specificity, positive predictive value (PPV), and negative predictive value (NPV) of lobar localization of MAP, QPET, MAP+QPET, and MAP/QPET for Engel I seizure outcome

	Sensitivity	Specificity	PPV	NPV
MAP	**64.4%**	**69.2%**	**78.3%**	**52.9%**
(95% CI)	(0.49–0.78)	(0.48–0.86)	(0.62–0.90)	(0.35–0.70)
QPET	**73.3%**	**65.4%**	**78.6%**	**58.6%**
(95% CI)	(0.58–0.85)	(0.44–0.83)	(0.63–0.90)	(0.39–0.76)
MAP+QPET	**53.3%**	**88.5%**	**88.9%**	**52.3%**
(95% CI)	(0.38–0.68)	(0.70–0.98)	(0.71–0.98)	(0.37–0.68)
MAP/QPET	**86.7%**	**46.2%**	**73.6%**	**66.6%**
(95% CI)	(0.73–0.95)	(0.27–0.67)	(0.60–0.85)	(0.41–0.87)

CI confidence interval; *PPV* positive predictive value; *NPV* negative predictive value

Table 3 Correlation analysis between surgical outcome and MAP, QPET, MAP+QPET, MAP/QPET concordant or non-concordant with cortical resection

	Engel I ($n=45$)	Engel II–IV ($n=26$)	P
MAP			**0.006****
Concordant with resection	29	8	
Non-concordant with resection	16	18	
QPET			**0.001****
Concordant with resection	33	9	
Non-concordant with resection	12	17	
MAP+QPET			**< 0.001*****
Concordant with resection	24	3	
Non-concordant with resection	21	23	
MAP/QPET			**0.002****
Concordant with resection	39	14	
Non-concordant with resection	6	12	

P was test by chi-square test, **$P < 0.01$, *** $P < 0.001$

patients. Among them, 33 patients achieved Engel I seizure outcomes, and nine patients with Engel II–IV seizure outcomes. QPET found no apparent hypometabolism in five patients and localized but non-concordant with surgical resection in 29 patients, of whom 12 patients achieved Engel I seizure outcome and 17 patients with Engel II–IV seizure outcome. The sensitivity of QPET was 73.30%, specificity was 65.4%, PPV was 78.6%, and NPV was 58.6% (Table 2). The region determined by QPET concordant with surgical resection was associated with favorable seizure outcomes compared to the ones non-concordant with surgical resection ($P=0.001$) (Table 3).

Fifteen patients had concordant QPET results but non-concordant MAP results with cortical resection, of whom 10 patients received Engel I surgical outcome. Eleven patients had concordant MAP but non-concordant QPET results with cortical resection, of whom six patients received Engel I surgical outcome. There was a significant difference between MAP and QPET for concordance with cortical resection ($\chi2=4.79$, $P=0.029$) (Table 4).

Figure 1 shows four representative cases with presurgical imaging evaluation and postsurgical CT.

MAP+QPET

Twenty seven patients the regions located by the combination of MAP+QPET were concordant with surgical resection, among them, 24 patients achieved Engel I surgical

outcome and three patients still with ongoing seizures. One or both of the combined tests were non-concordant with the surgical resection in 21 patients with Engel I seizure outcome and in 23 patients with Engel II–IV seizure outcome. The sensitivity of MAP+QPET was 53.3%, specificity was 88.5%, PPV was 88.9%, and NPV was 52.3% (Fig. 2). The region determined by MAP+QPET concordant with surgical resection was associated with favorable seizure outcomes compared to the ones non-concordant with cortical resection ($P<0.001$) (Table 3).

MAP/QPET

The MAP/QPET was concordant with cortical resection in 39 patients with Engel I surgical outcome and 14 patients with Engel II–IV surgical outcome. Eighteen patients the regions located by the combination of MAP/QPET were non-concordant with surgical resection, among them, six patients achieved Engel I surgical outcome and 12 patients still with ongoing seizures. The sensitivity of MAP/QPET was 86.7%, specificity was 46.2%, PPV was 73.6%, and NPV was 66.6% (Fig. 2). The region determined by MAP/QPET concordant with surgical resection was associated with favorable seizure outcomes compared to the ones non-concordant with cortical resection ($P=0.002$) (Table 3). The correction between surgical outcome and MAP or QPET localization results is shown in Fig. 3.

Table 4 The difference between MAP and QPET for concordance with cortical resection

|		QPET		$\chi2$	P
		Concordant	Non-concordant		
MAP	Concordant	27	11	4.70	**0.029***
	Non-concordant	15	18		

P was test by chi-square test. * $P < 0.05$

Fig. 1 Examples of four patients with QPET and MAP results and surgical resection. Case 1, QPET and MAP indicated the region in the left frontal lobe. The patients achieved seizure-free at 1 year. Case 2, QPET showed no definitive hypometabolism, and MAP indicated the region in the left frontal lobe. The patients achieved seizure-free at 1 year. Case 3, QPET showed hypometabolism in the left temporal lobe and hippocampus, and MAP was negative. The patients achieved seizure-free at 1 year. Case 4, both QPET and MAP were negative, surgical resection was performed on the left temporal lobe based on other preoperative evaluation, and the patient was Engel III at 1 year
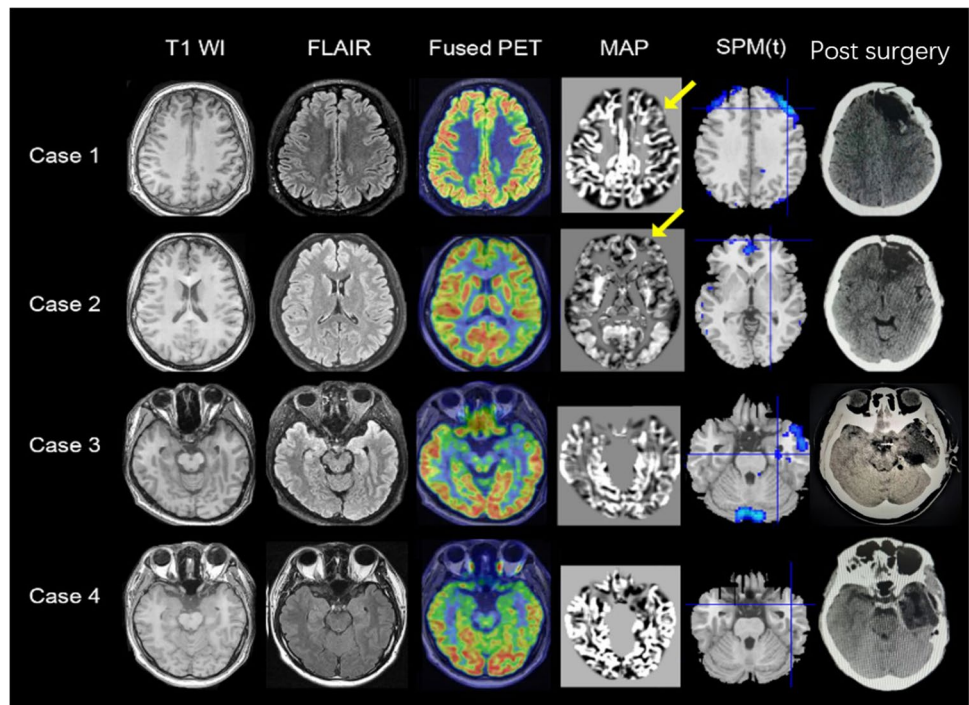
Fig. 2 The ROC curves of MAP + QPET and MAP/QPET. For the combination of MAP/QPET, defined as one or both test(s) concordant with surgical resection, had increased sensitivity but reduced specificity relative to individual tests; the area under curve was 0.664, 95% CI (0.554–0.774). For the combination of MAP + QPET, defined as two tests concordant with surgical resection, had reduced sensitivity but increased specificity relative to individual tests; the area under curve was 0.709, 95% CI (0.612–0.806)
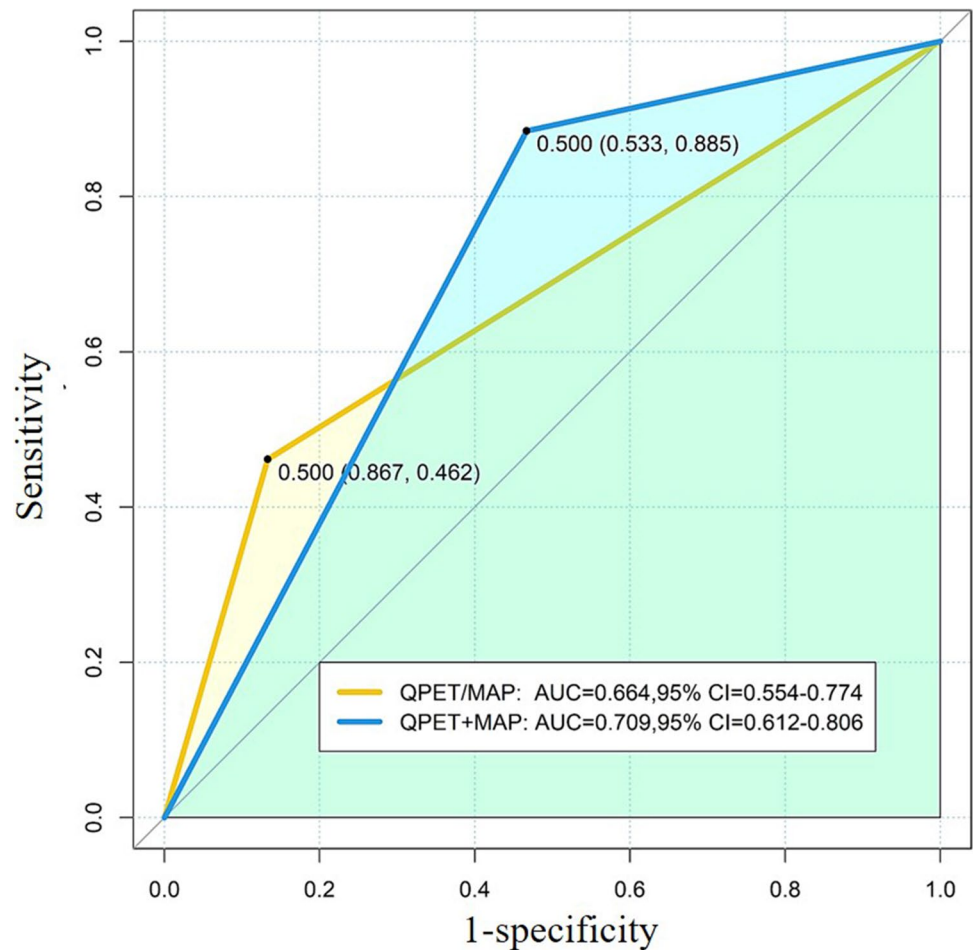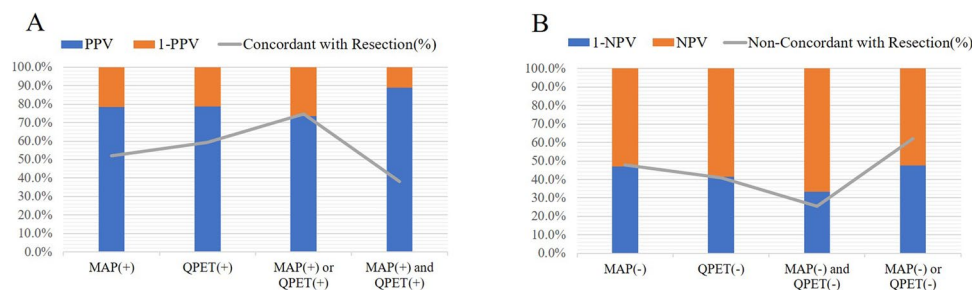
Fig. 3 Correction between surgical outcome and MAP or QPET localization results. In the regions located by the combination of MAP + QPET concordant with surgical resection in 27 patients, among them, 88.9% of patients achieved Engel I surgical outcome.

However, the positive ratio of QPET (+) and MAP (+) was only 38.0%; for 18 patients with MAP (-) and QPET (-), but surgery still performed, 66.7% were Engel II–IV at 1-year follow-up

Within eighteen patients with MAP or QPET non-concordant with cortical resection, 12 patients did not receive seizure-free outcomes, the baseline measurements of those patients presented in the supplement Table 1. Other six patients who received seizure-free outcomes are presented in the supplement Table 2. The operative pathologies included the following: 12 patients were FCD (7 patients were FCD I, four patients were FCD II, and one patient was FCD III), one patient was ulegyria, one patient was hippocampus sclerosis, and four patients were negative.

Discussion

We calculated sensitivity, specificity, PPV, and NPV of MAP and QPET in patients with Engel I seizure outcome following cortical resection and assessed the association between localization of diagnostic test relative to cortical resection and surgical outcomes. We found that QPET has a superior sensitivity than MAP. The combined MAP + QPET obtained from a simultaneous PET/MRI scanner may improve the specificity of the diagnostic tests in EZ localization coupled with the preferable surgical outcome in MRI-negative epilepsies.

MAP is increasingly used to complement the visual analysis and elucidate structural epileptogenic lesions in preoperative evaluation. Wang et al. performed a retrospective study in 150 "non-lesion" epilepsies patients and showed that MAP positive areas were detectable in 65 patients [3]. Lin et al. showed MAP positive regions were found in 82 of the 104 patients [14]. Our retrospective study detected candidate MAP positive regions in 70.4% of patients. The differences in detection rates may be explained by non-uniform inclusion criteria of MRI-negative patients. The absence of a lesion on MRI has consistently been shown as a predictor for surgical failure [17, 18]. MAP results turned some cases from MRI-negative to MRI-positive. These patients are more likely to become seizure-free following cortical resection of

the subtle lesion. Previous studies showed complete resection of the MAP positive region correlated positively with seizure-free outcomes [3, 5, 14]. Our study also found that MAP positive regions concordant with cortical resection were associated with a favorable surgical outcome compared to the non-concordant ones. Those results indicated that the MAP positive region may be a potential epileptogenic lesion, since MAP is only a postprocessing method without incurring any additional cost or risk to patients, and may be applied to standard preoperative evaluation.

Although previous studies demonstrated visual analysis yielded similar findings to SPM analysis of abnormal metabolism in localization-related epilepsy [13, 19], a quantitative analysis may be more subjective and identify more areas of abnormal metabolism. Tomás et al. showed QPET sensitivity and specificity were both 95% in temporal lobe epilepsy (TLE) patients and 80% and 95% respectively in extratemporal epilepsy (ETLE) patients in a study including 130 epilepsy patients [20]. Lin et al. evaluated QPET thresholds of four standard deviations (SDs) to identify the optimal threshold for QPET analysis, and they demonstrated that the QPET SD threshold of + 2 showed the best combination of positive rate (55%), sensitivity (68%), and specificity (88%) [14]. In this study, $P < 0.05$ without correction for multiple comparisons was considered statistically significant in ^{18}F-FDG PET images processed. Since the beginning, we have performed two thresholds ($P < 0.05$; $P < 0.01$) for multiple comparisons; however, near 30% of patients showed no apparent hypometabolism on SPM (t) maps for $P < 0.01$ without correction. The sensitivity was similar to the previous study. The specificity was lower, and the specificity was extremely limited in the retrospective study that QPET did not guide surgical resections.

The combined MAP + QPET increased the specificity of the tests and therefore reduced the number of false-positive tests, whereas the MAP/QPET tests increased the sensitivity and therefore reduced the number of false-negative tests for Engel I surgical outcome. Similar to other

multimodality imaging studies [21], although they chose different modalities, all indicated that if one diagnostic test was non-localizing, a second diagnostic test could increase the likelihood of localizing the epileptogenic zone. Ding et al. [22] have shown that presurgical evaluation by co-registration of ^{18}F-FDG PET and MRI could improve the identification of the epileptogenic onset zone and may further guide surgical and improve the outcome in the refractory ETLE patients with normal MRI. Desarnaud et al. [23] integrated electroclinical data and PET/MRI co-registration and obtained a high localizing value of 83% in FCD patients. Lin et al. [14] utilized QPET analysis to complement MAP to facilitate automated identification of subtle FCD, revealing the usefulness of QPET-MAP analysis in detecting potentially epileptogenic lesions and finding the association between the resection of the QPET-MAP positive regions and good seizure outcome. In the present study, the PET and MRI images in our study were obtained from a simultaneous PET/MRI scanner, whether MAP + QPET or MAP/QPET; the abnormalities concordant with cortical resection were significantly associated with seizure-free outcomes.

Another important feature demonstrated in our study was the complementary role of QPET and MAP in EZ localization. MAP positive regions concordant with cortical resection were associated with favorable seizure outcomes. However, nearly half of patients showed more than one MAP positive region or MAP negative. In this study, for the 15 patients with multiple candidate MAP regions, QPET helped 6 of them to exclude candidate MAP positive regions caused by imaging artifacts, misregistration, or nonepileptic variants. For the 21 patients with a negative MAP, QPET showed additional sensitivity detected potential EZ in 15 patients. The hypometabolism shown on PET often extended beyond the epileptogenic region and hence hardly yielded a precise surgical margin. The broader localization of QPET could be complemented by the more precise localization of potential structural abnormalities, MAP helped to identify 5 patients in the present study. Mendes Coelho et al. [24] demonstrated QPET had critical value for patients with subtle MRI findings. Another study showed combined features assisted by machine learning from MRI and PET outperformed in FCD localization [25]. Those published studies, along with our results, suggest that correlating findings from functional and structural methods improve the identification of EZ and surgical outcomes.

The main limitation is that this was a retrospective study. All patients received comprehensive preoperative evaluations, including symptomatology, EEG/MEG, and intracardial EEG. The QPET and MAP results may not direct surgical resection, so the specificity of diagnostic tests in epileptic foci localization may be limited. Secondly, the performance of MAP, PET, and combining them may be biased because only the patients with surgical treatment were included. The performance was not evaluated in patients who did not undergo surgical treatment in the present study. Thirdly, simultaneous review of the MR and PET images was also an advantage of simultaneous PET/MRI. However, the image interpretation was read separately.

Conclusions

In conclusion, QPET has a superior sensitivity than MAP, while the combined MAP + QPET obtained from a simultaneous PET/MRI scanner may improve the specificity of the diagnostic tests in EZ localization coupled with the preferable surgical outcome in MRI-negative epilepsies.

Declarations

Research involving human participants and/or animals The research involved human participants. This retrospective study was permitted by the Research Ethics Committee of the Capital Medical University of Xuanwu hospital.

Consent to participate All patients gave written informed consent prior to enrollment in this study.

Conflict of interest The authors declare no competing interests.

References

1. Malmgren K, Krýsl D. Epilepsy: long-term outcomes in MRI-negative patients with epilepsy. Nat Rev Neurol. 2017;13:132–3.
2. Pellinen J, Kuzniecky R, Doyle W, Devinsky O, Dugan P. MRI-negative PET-negative epilepsy long-term surgical outcomes: a single-institution retrospective review. Epilepsy Res. 2020;67:106481.
3. Wang ZI, Jones SE, Jaisani Z, Najm IM, Prayson RA, Burgess RC, et al. Voxel-based morphometric magnetic resonance imaging (MRI) postprocessing in MRI-negative epilepsies. Ann Neurol. 2015;77:1060–75.
4. Sun K, Ren Z, Yang D, Wang X, Yu T, Ni D, et al. Voxel-based morphometric MRI post-processing and PET/MRI co-registration reveal subtle abnormalities in cingulate epilepsy. Epilepsy Res. 2021;171:106568.

5. Wagner J, Weber B, Urbach H, Elger CE, Huppertz HJ. Morphometric MRI analysis improves detection of focal cortical dysplasia type II. Brain. 2011;134:2844–54.

6. Kim YK, Lee DS, Lee SK, Kim SK, Chung CK, Chang KH, et al. Differential features of metabolic abnormalities between medial and lateral temporal lobe epilepsy: quantitative analysis of (18) F-FDG PET using SPM. J Nucl Med. 2003;44:1006–12.

7. Liu F, Ruan W, Deng X, Song Y, Song W, Hu F, et al. Efficacy of delayed ^{18}F-FDG hybrid PET/MRI for epileptic focus identification: a prospective cohort study. Eur J Nucl Med Mol Imaging. 2021;48:293–301.

8. Zhu Y, Feng J, Wu S, Hou H, Ji J, Zhang K, et al. Glucose metabolic profile by visual assessment combined with statistical parametric mapping analysis in pediatric patients with epilepsy. J Nucl Med. 2017;58:1293–9.

9. von Oertzen TJ. PET and ictal SPECT can be helpful for localizing epileptic foci. Curr Opin Neurol. 2018;31:184–91.

10. Ponisio MR, Zempel JM, Day BK, Eisenman LN, Miller-Thomas MM, Smyth MD, et al. The role of SPECT and PET in epilepsy. AJR Am J Roentgenol. 2021;216:759–68.

11. Mayoral M, Marti-Fuster B, Carreño M, Carrasco JL, Bargalló N, Donaire A, et al. Seizure-onset zone localization by statistical parametric mapping in visually normal (18) F-FDG PET studies. Epilepsia. 2016;57:1236–44.

12. Peter J, Houshmand S, Werner TJ, Rubello D, Alavi A. Applications of global quantitative 18F-FDG-PET analysis in temporal lobe epilepsy. Nucl Med Commun. 2016;37:223–30.

13. Kumar A, Juhász C, Asano E, Sood S, Muzik O, Chugani HT. Objective detection of epileptic foci by ^{18}F-FDG PET in children undergoing epilepsy surgery. J Nucl Med. 2010;51:1901–7.

14. Lin Y, Fang YD, Wu G, Jones SE, Prayson RA, Moosa ANV, et al. Quantitative positron emission tomography-guided magnetic resonance imaging postprocessing in magnetic resonance imaging-negative epilepsies. Epilepsia. 2018;59:1583–94.

15. Blümcke I, Thom M, Aronica E, Armstrong DD, Vinters HV, Palmini A, et al. The clinicopathologic spectrum of focal cortical dysplasias: a consensus classification proposed by an ad hoc Task Force of the ILAE Diagnostic Methods Commission. Epilepsia. 2011;52:158–74.

16. Engel JJ, Van Ness NP, Rasmussen TB, Ojemann LM. Outcome with respect to epileptic seizures. In: Engel JJ, editor. Surgical treatment of the epilepsies. 2nd ed. New York: Raven Press; 1993. p. 609–21.

17. Ryvlin P, Rheims S. Predicting epilepsy surgery outcome. Curr Opin Neurol. 2016;29:182–8.

18. Krucoff MO, Chan AY, Harward SC, Rahimpour S, Rolston JD, Muh C, et al. Rates and predictors of success and failure in repeat epilepsy surgery: a meta-analysis and systematic review. Epilepsia. 2017;58:2133–42.

19. Juhász C, John F. Utility of MRI, PET, and ictal SPECT in presurgical evaluation of non-lesional pediatric epilepsy. Seizure. 2020;77:15–28.

20. Tomás J, Pittau F, Hammers A, Bouvard S, Picard F, Vargas MI, et al. The predictive value of hypometabolism in focal epilepsy: a prospective study in surgical candidates. Eur J Nucl Med Mol Imaging. 2019;46:1806–16.

21. Widjaja E, Shammas A, Vali R, Otsubo H, Ochi A, Snead OC, et al. FDG-PET and magnetoencephalography in presurgical workup of children with localization-related non-lesional epilepsy. Epilepsia. 2013;54:691–9.

22. Ding Y, Zhu Y, Jiang B, Zhou Y, Jin B, Hou H, et al. ^{18}F-FDG PET and high-resolution MRI co-registration for pre-surgical evaluation of patients with conventional MRI-negative refractory extra-temporal lobe epilepsy. Eur J Nucl Med Mol Imaging. 2018;45:1567–72.

23. Desarnaud S, Mellerio C, Semah F, Laurent A, Landre E, Devaux B, et al. ^{18}F-FDG PET in drug-resistant epilepsy due to focal cortical dysplasia type 2: additional value of electroclinical data and co-registration with MRI. Eur J Nucl Med Mol Imaging. 2018;45:1449–60.

24. Mendes Coelho VC, Morita ME, Amorim BJ, Ramos CD, Yasuda CL, Tedeschi H, et al. Automated online quantification method for ^{18}F-FDG positron emission tomography/CT improves detection of the epileptogenic zone in patients with pharmaco-resistant epilepsy. Front Neurol. 2017;8:453.

25. Tan YL, Kim H, Lee S, Tihan T, Ver Hoef L, Mueller SG, et al. Quantitative surface analysis of combined MRI and PET enhances detection of focal cortical dysplasia. Neuroimage. 2018;166:10–8.